Available online at www.sciencedirect.com
ScienceDirect
Mendeleev Commun., 2020, **30**, 639–641

Mendeleev
Communications

Synthesis and characterization of triethanolamine complexes with cobalt(II) and zinc(II) cinnamates

Yulia A. Kondratenko,[a] Valery L. Ugolkov,[a] Dmitry Yu. Vlasov[b] and Tatyana A. Kochina*[a]

[a] *I. V. Grebenshchikov Institute of Silicate Chemistry, Russian Academy of Sciences, 199034 St. Petersburg, Russian Federation. E-mail: t-kochina@mail.ru*
[b] *St. Petersburg State University, 199034 St. Petersburg, Russian Federation*

DOI: 10.1016/j.mencom.2020.09.029

New hydrometallatranes, *viz.* complexes of triethanolamine with Zn^{II} and Co^{II} cinnamates, have been synthesized and characterized by IR spectroscopy, ESI mass spectrometry, elemental and thermal analyses. The structure of cobalt complex has been solved using single-crystal X-ray diffraction. The compounds synthesized and their analogues have been tested for antimicrobial activity.

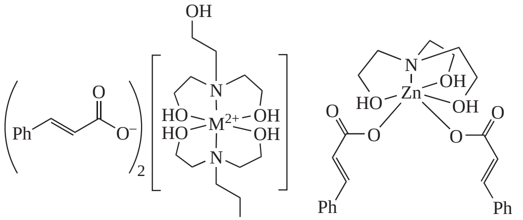

M = Co, Zn

Keywords: zinc complex, cobalt complex, cinnamate, triethanolamine, atrane, crystal structure, thermal stability, antimicrobial activity.

Over the past three decades atranes as intracomplex compounds of triethanolamine (TEA) have proven biologically active for use in medicine, cosmetology, agriculture and other areas.[1–5] Hydrometallatranes represent compounds of atrane class, which include cationic mononuclear complexes,[6–8] mononuclear mixed-ligand ones as well as bi- and polynuclear mixed-ligand complexes of metal salts containing one or more deprotonated hydroxyethyl groups of TEA.[9–12] Among hydrometallatranes, low-toxic substances with immunomodulating properties[13,14] and new potential agent, namely zincatrane, for the prevention of sclerotic lesions in blood vessels[15] were identified. Besides, hydrometallatranes are effectively used as catalysts or catalyst precursors for various chemical reactions, most of which are of interest to the industry.[16–18]

Cinnamic acid (CinH) and its derivatives attract attention due to their anticancer, antioxidant, antimicrobial, acaricidal and cytotoxic properties.[19–21] Cinnamates are employed in industry as graphics materials, lubricants and plasticizers, in particular alkyl cinnamates are used as perfume essence, soap and flavouring components.[22,23] They are potential food preservatives as well as antimicrobial agents against human pathogenic bacteria and fungi.[24] Cinnamate derivatives represent a good alternative to conventional biocides, because they behave as environmentally friendly compounds.

The objective of this work was to obtain and characterize new biologically active hydrometallatranes based on TEA, CinH and biogenic metals such as zinc and cobalt. Complexes $[Co(TEA)_2](Cin)_2$ **1**, $[Zn(TEA)(Cin)_2]$ **2** and $[Zn(TEA)_2](Cin)_2$ **3** were synthesized by reaction of TEA with cobalt(II) and zinc(II) cinnamates at molar ratios of 1 : 1 and 2 : 1 in methanol.† In fact, the reactions of zinc(II) cinnamate with TEA at ratios of 1 : 1 and 1 : 2 leads to complexes **2** and **3** of different structures, respectively. This was confirmed by elemental analysis, IR spectroscopy and mass spectrometry. The ESI mass spectrum of complex **2** shows peaks of the following ions: $[TEA–H]^+$, $[TEA–Na]^+$, $[Zn(TEA^–)]^+$,‡ $[Zn(TEA)(Cin)]^+$ and $[Zn_2(TEA^–)(Cin)_2]^+$.† In the ESI mass spectrum of complex **3**, only two peaks belonging to ion fragments $[TEA–H]^+$ and $[Zn(TEA^–)_2–H]^+$ were identified. Based on the data obtained, it can be assumed that the reaction of zinc(II) cinnamate with TEA at a molar ratio of 1 : 1 leads to the mixed-ligand complex of an estimated composition $[Zn(TEA)(Cin)_2]$. Increase in the amine content of the reaction mixture (molar ratio of 1 : 2) significantly affects the structure of the complex, which leads to the cationic mononuclear coordination compound consisting of $[Zn(TEA)_2]^{2+}$ cations and cinnamate anions. Importantly, the reaction of cobalt(II) cinnamate with TEA both at a ratio of 1 : 1 and 1 : 2 affords the same complex **1**, whose structure was unambiguously established by single crystal X-ray diffraction (Figure 1).

In the IR spectra of complexes **1**–**3**, bands of stretching vibrations for the OH groups of TEA are observed in the region of 3430–3270 cm^{-1}. The intense band at 1640 cm^{-1} is associated with stretching vibrations of the C=C group conjugated with phenyl group of cinnamate anion. The stretching vibrations of carboxylate groups of the anions appear as two bands in the region of 1580–1550 and 1410–1380 cm^{-1} (Table 1).

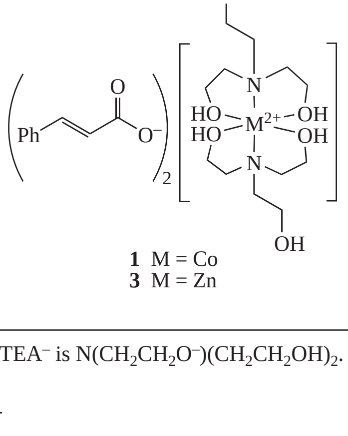

1 M = Co
3 M = Zn

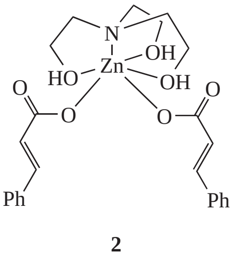

2

---

† For details, see Online Supplementary Materials.

‡ $TEA^–$ is $N(CH_2CH_2O^–)(CH_2CH_2OH)_2$.

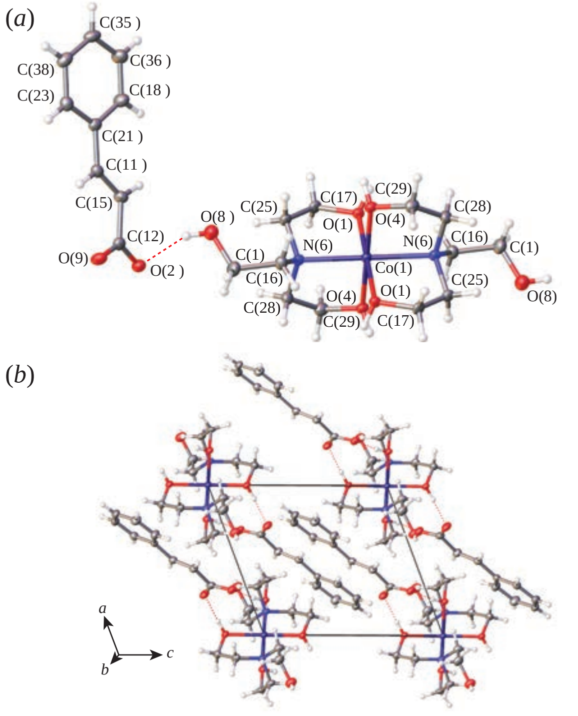

Figure 1 (*a*) Molecular structure and (*b*) crystal structure of complex **1**, viewed along the *a* axis. Dashed lines indicate the intermolecular hydrogen bonding. Distances (Å): O(4)–H 0.84, O(4)H···O(9) 1.72, O(4)···O(9) 2.565(3), O(1)–H 0.85, O(1)H···O(2) 1.74, O(1)···O(2) 2.585(3), O(8)–H 0.82, O(8)H···O(2) 2.14, O(8)···O(2) 2.878(4). Angles (°): O(4)–H···O(9) 175(3), O(1)–H···O(2) 171(3), O(8)–H···O(2) 150(0).

Table 1 The assignment of the bands from stretching vibrations[a] in complexes **1**–**3**.

Complex	ν(OH)	ν(CH), [ν(CH$_2$)]/cm^{-1}	ν(C=C), [ν(CAr)]/cm^{-1}	ν_{as}(COO)/ cm^{-1}	ν_s(COO)/ cm^{-1}
1	3350 (s, br)	3150 (w) 2970 (w) 2890 (w) [2830 (w)]	1640 (m) [1560 (m)] 1500 (m) [1450 (m)]	1580 (m)	1380 (s)
2	3430 (w) 3350 (w) 3280 (w)	3060 (w) 3030 (w) 2970 (w) [2900 (w)]	1640 (s) 1500 (m) [1450 (m)]	1550 (s)	1410 (s)
3	3350 (s) 3270 (m)	3150 (m) 3080 (w) 3020 (w) 2930 (w) 2900 (w)	1640 (s) 1490 (m) [1450 (m)]	1560 (s)	1410 (s)

[a] s, m, w and br indicate strong, medium, weak and broadened, respectively.

According to single crystal X-ray diffraction data,[§] complex **1** is a cationic mononuclear one and consists of [Co(TEA)$_2$]$^{2+}$ cations as well as cinnamate anions (Figure 2). Cations are formed by a metal atom coordinated by two TEA ligands through two oxygen atoms and the nitrogen atom. The third hydroxyethyl moiety of TEA does not participate in complexation with the metal atom, *i.e.*, TEA acts as a tridentate ligand. The coordination polyhedron of the cobalt atom corresponds to a distorted octahedron CoN$_2$O$_4$. The bond lengths Co(1)–N(6), Co(1)–O(1) and Co(1)–O(4) are 2.158(2), 2.0832(19) and 2.0926(19) Å, respectively. Complete geometric parameters, namely bond lengths, valence and torsion angles, for complex **1** are presented in Online Supplementary Materials.

The [Co(TEA)$_2$]$^{2+}$ cations and anions are arranged in columns along the *b*-axis [Figure 2(*b*)]. Each oxygen atom of the hydroxyethyl moiety of TEA forms hydrogen bonds with anions, acting as a proton donor. Cations inside the columns, which form hydrogen bonds with the oxygen atom O$_2$ of cinnamate anion, are arranged in chains. Herewith, the neighbouring cation columns arranged along *b*-axis are not bound by hydrogen bonds to each other.

The thermal stability of compounds **1**–**3** was studied by complex thermal analysis in the temperature range of 40–600 °C. Thermogravimetric curves of complexes **1**–**3** are characterized by two or three noticeable steps of mass loss. The beginning of the thermal decomposition of compounds **1**–**3** occurred almost immediately after complete melting of the sample, which appeared in the differential scanning calorimetry (DSC) curve as symmetrical endothermic effect with a maximum in the temperature range of 122–146 °C. Thermal decomposition of complex **1**[¶] proceeded through two steps of mass loss in the temperature range of 159–246 °C (–38.15%) and 302–461 °C (–39.91% of mass). At the first step, weak endothermic effect with a maximum at 198 °C in the DSC curve and a slight increase in the level of H$_2$O and CO$_2$ in the IC curves were observed. The burning process of compound **1** proceeded actively at the second step. In the temperature range of 302–461 °C, strong exothermic effect appeared in the DSC curve with two maxima at 384 and 429 °C when water and carbon dioxide were extensively released.

The thermal decomposition of complexes **2** and **3** proceeded in a similar way, *i.e.*, after the melting three noticeable steps of mass loss occurred. In the DSC curves of compounds **2** and **3**, small exothermic effects were observed with maxima at 345 °C (complex **2**), 314 and 338 °C for complex **3**, accompanied by strong release of water and carbon dioxide in the IC curves. Strong exothermic effects with maxima at 500 °C for complex **2** and 489 °C for complex **3** were observed at the third decomposition step, which were probably related to the carbonation process of the organic residue. Finally, compounds **2** and **3** were transformed into yellowish zinc oxide. The decomposition of cobalt(II) complex **1** probably resulted in dark gray mixed oxide Co$_3$O$_4$.

Since CinH derivatives have a pronounced antimicrobial activity,[19–21,24] one may expect that complexes **1**–**3** can demonstrate a noticeable effect. Thus, their antimicrobial activity[††] along with other TEA and CinH analogues was studied against bacteria *Escherichia coli*, *Staphylococcus aureus*, *Mycobacterium smegmatis* as well as fungi *Candida albicans* and *Aspergillus niger*. Triethanolammonium salt of CinH and two TEA complexes,

---

[§] *Crystal data for* **1**. C$_{30}$H$_{44}$CoN$_2$O$_{10}$, $M = 651.60$, triclinic, space group $P\bar{1}$, $a = 9.0046(16)$, $b = 9.7488(16)$ and $c = 10.1181(18)$ Å, $\alpha = 107.768(16)$, $\beta = 103.619(16)$ and $\gamma = 106.790(15)$°, $V = 757.1(3)$ Å^3, $Z = 1$, $\mu = 4.955$ mm^{-1}, $T = 100(2)$ K, 5327 reflections measured, 2866 independent reflections ($R_{int} = 0.0471$), $R[F^2 > 2\sigma(F^2)] = 0.0494$, $wR(F^2) = 0.1300$, GOF = 1.055. The single crystal X-ray diffraction experiment was performed using an Oxford Diffraction SuperNova diffractometer with monochromated CuKα radiation. Structure **1** was solved by direct methods and refined using a SIR2011 program.[25] The carbon-bound H atoms were placed in calculated positions and included in the refinement according to the ‘riding’ model approximation with U_{iso}(H) set to 1.2U_{eq}(C) and C–H 0.96 Å for the CH groups as well as with U_{iso}(H) set to 1.2U_{eq}(C) and C–H 0.97 Å for the CH$_2$ groups. All H atoms bound to O atoms were located in the difference Fourier map. Empirical absorption correction was carried out using a CrysAlis^{Pro} program complex[26] with spherical harmonics implemented in a SCALE3 ABS PACK scaling algorithm.

CCDC 1979662 contains the supplementary crystallographic data for this paper. These data can be obtained free of charge from The Cambridge Crystallographic Data Centre *via* http://www.ccdc.cam.ac.uk.

[¶] For details, see Online Supplementary Materials.

[††] Antimicrobial activity was investigated against the standard strains from the collection of the Department of Microbiology, Virology and Immunology of I. P. Pavlov First St. Petersburg State Medical University. The minimal inhibitory concentration was defined as the lowest concentration of an antimicrobial agent at which there was no visible growth of the microbe. Minimal inhibitory concentrations were determined by the tube dilution method.[27,28]

Table 2 Antimicrobial activity of complexes **1**–**3** and other TEA compounds.

Compound	Minimum inhibitory concentration/μg ml^{-1}				
	E. coli	*S. aureus*	*M. smegmatis*	*C. albicans*	*A. niger*
1	>100	25	>100	>100	100
2	>100	25	>100	>100	>100
3	>100	50	>100	>100	>100
[TEAH](Cin)	>100	25	>100	>100	>100
[Zn(TEA)$(H_2O)_2$]$SO_4\cdot H_2O$	>100	12.5	12.5	>100	>100
[Cu_2(TEA)$_2$(Cin)$_2$]$\cdot H_2O$	>100	25	>100	>100	>100

namely, [Zn(TEA)$(H_2O)_2$]$SO_4\cdot H_2O$[9] and [Cu_2(TEA)$_2$(Cin)$_2$]$\cdot H_2O$[10] were selected. All the studied TEA compounds (Table 2) showed high activity against the bacterium *S. aureus* (MIC = 12.5–50 μg ml^{-1}). Note that according to the known data the MIC values for methyl cinnamate, butyl cinnamate and methyl *p*-methoxycinnamate against *S. aureus* exceed 1000 μg ml^{-1}.[24,29] Thus, here the effect can be explained by the presence of TEA fragment. Among the compounds studied, [Zn(TEA)$(H_2O)_2$]$SO_4\cdot H_2O$ complex showed the highest activity against *S. aureus*. This Zn^{II} complex is also the only compound that demonstrated high activity against *M. smegmatis*.

However, among the compounds explored, only complex **1** showed activity against the fungus *A. niger* with MIC = 100 μg ml^{-1}. In this regard, we investigated in more detail the ability of complex **1** to inhibit the growth and development of micromycetes.[‡‡] Thus, *A. niger*, *Cladosporium cladosporioides* and *Penicillium brevicompactum* as three fungal species that can cause the biodestruction of various materials were included in the test. The effect of complex **1** was compared with the action of triethanolammonium salt of CinH as well as TEA complexes in order to explore the influence of the corresponding components on the observed activity. The results were evaluated on a five-point scale and demonstrated a different degree of influence of complex **1** and [TEAH](Cin) on the development of micromycetes as biodestructors of materials. [TEAH](cin) had a negligible impact on the growth and development of fungi of the three types. In contrast to the salt, cobalt(II) complex **1** showed the maximum effect and inhibited the growth of all the tested micromycetes.

Thus, Co^{II} complex **1** demonstrated high activity against micromycetes as the main destructors of materials and could be recommended as a promising biocidal additive to protective materials and coatings.

In conclusion, three new triethanolamine complexes with cobalt(II) and zinc cinnamates were obtained and characterized. The cationic Co^{II} complex **1** shows high activity against micromycetes, which cause biodegradation of materials, and can be recommended as a promising biocidal additive.

The scientific research was performed at the Centre for Optical and Laser Materials Research, Chemical Analysis and Materials Research Centre, Centre for X-ray Diffraction Studies and Magnetic Resonance Research Centre of the Research park of St. Petersburg State University.

Online Supplementary Materials

Supplementary data associated with this article can be found in the online version at doi: 10.1016/j.mencom.2020.09.029.

References

1 M. G. Voronkov and V. P. Baryshok, *Herald Russ. Acad. Sci.*, 2010, **80**, 514 (*Vestn. Ross. Akad. Nauk*, 2010, **80**, 985).

2 M. G. Voronkov, O. P. Kolesnikova, M. M. Rasulov and A. N. Mirskova, *Pharm. Chem. J.*, 2007, **41**, 244 [*Khim.-Farm. Zh.*, 2007, **41** (5), 13].

3 M. G. Voronkov and V. P. Baryshok, *Pharm. Chem. J.*, 2004, **38**, 3 [*Khim.-Farm. Zh.*, 2004, **38** (1), 5].

4 S. N. Adamovich, E. N. Oborina and I. A. Ushakov, *Mendeleev Commun.*, 2019, **29**, 688.

5 V. I. Smirnov, E. A. Zelbst, G. A. Kuznetzova and I. V. Sterkhova, *Mendeleev Commun.*, 2018, **28**, 278.

6 I. Ignatyev, Y. Kondratenko, V. Fundamensky and T. Kochina, *Transition Met. Chem.*, 2018, **43**, 127.

7 Y. Topcu, V. T. Yilmaz and C. Thöne, *Acta Crystallogr., Sect. E: Crystallogr. Commun.*, 2001, **57**, m600.

8 A. N. Mirskova, S. N. Adamovich, R. G. Mirskov and U. Schilde, *Chem. Centr. J.*, 2013, **7**, 34.

9 Y. Kondratenko, V. Fundamensky, I. Ignatyev, A. Zolotarev, T. Kochina and V. Ugolkov, *Polyhedron*, 2017, **130**, 176.

10 Y. Kondratenko, A. A. Zolotarev, I. Ignatyev, V. Ugolkov and T. Kochina, *Transition Met. Chem.*, 2020, **45**, 71.

11 R. M. Escovar, J. H. Thurston, T. Ould-Ely, A. Kumar and K. H. Whitmire, *Z. Anorg. Allg. Chem.*, 2005, **631**, 2867.

12 Y. Yu. Karabach, A. M. Kirillov, M. F. C. Guedes da Silva, M. N. Kopylovich and A. J. L. Pombeiro, *Cryst. Growth Des.*, 2006, **6**, 2200.

13 O. P. Kolesnikova, A. N. Mirskova, S. N. Adamovich, G. A. Kuznetsova, O. T. Kudaeva, I. A. Goldina, I. V. Safronova, R. G. Mirskov, K. V. Gaidul and M. G. Voronkov, *Byulleten' Sibirskogo Otdeleniya Rossiiskoi Akademii Meditsinskikh Nauk*, 2009, **6**, 73 (in Russian).

14 S. N. Adamovich and E. N. Oborina, *Russ. Chem. Bull., Int. Ed.*, 2019, **68**, 1723 (*Izv. Akad. Nauk, Ser. Khim.*, 2019, 1723).

15 K. A. Abzaeva, M. M. Rasulov and I. V. Zhigacheva, *Russ. Chem. Bull., Int. Ed.*, 2019, **68**, 1122 (*Izv. Akad. Nauk, Ser. Khim.*, 2019, 1122).

16 A. M. Kirillov, M. N. Kopylovich, M. V. Kirillova, M. Haukka, M. F. C. Guedes da Silva and A. J. L. Pombeiro, *Angew. Chem.*, 2005, **117**, 4419.

17 D. Wang, D. Kuang, F. Zhang, S. Tang and W. Jiang, *Eur. J. Org. Chem.*, 2014, 315.

18 S. N. Adamovich, R. G. Mirskov and A. N. Mirskova, *Russ. Chem. Bull., Int. Ed.*, 2015, **64**, 2275 (*Izv. Akad. Nauk, Ser. Khim.*, 2015, 2275).

19 L. Li, P. Zhao, J. Hu, J. Liu, Y. Liu, Z. Wang, Y. Xia, Y. Dai and L. Chen, *Eur. J. Med. Chem.*, 2015, **93**, 300.

20 G.-C. Yen, Y.-L. Chen, F.-M. Sun, Y.-L. Chiang, S.-H. Lu and C.-J. Weng, *Eur. J. Pharm. Sci.*, 2011, **44**, 281.

21 D.-D. Chen, B.-Y. Zhang, X.-X. Liu, X.-Q. Li, X.-J. Yang and L. Zhou, *Bioorg. Med. Chem. Lett.*, 2018, **28**, 1149.

22 L. M. Saavedra, D. Ruiz, G. P. Romanelli and P. R. Duchowicz, *Ecotoxicol. Environ. Saf.*, 2015, **122**, 521.

23 L. Shu and Y. Hongjun, *Eur. Chem. Bull.*, 2013, **2**, 76.

24 O. D. Stefanović, I. D. Radojević and L. R. Čomić, *Hem. Ind.*, 2015, **69**, 37.

25 M. C. Burla, R. Caliandro, M. Camalli, B. Carrozzini, G. L. Cascarano, C. Giacovazzo, M. Mallamo, A. Mazzone, G. Polidori and R. Spagna, *J. Appl. Crystallogr.*, 2012, **45**, 357.

26 *CrysAlis^{Pro}, Version 1.171.36.32*, Agilent Technologies, 2013.

27 *M07-A5. Methods for Dilution Antimicrobial Susceptibility Tests for Bacteria That Grow Aerobically*, 6th edn., NCCLS, Wayne, PA, 2000.

28 *M38-P. Reference Method for Broth Dilution Antifungal Susceptibility Testing of Conidium Forming Filamentous Fungi*, NCCLS, Wayne, PA, 1998.

29 M. J. Alves, I. C. F. R. Ferreira, H. J. C. Froufe, R. M. V. Abreu, A. Martins and M. Pintado, *J. Appl. Microbiol.*, 2013, **115**, 346.

Received: 6th April 2020; Com. 20/6189

[‡‡] See details in Online Supplementary Materials.